

## Phase relations and physical properties of $\text{Li}_{2r}\text{Mg}_{1-r}\text{Cu}_{2-r}\text{O}_{3-r+x}$

This article has been downloaded from IOPscience. Please scroll down to see the full text article.

1989 J. Phys.: Condens. Matter 1 611

(<http://iopscience.iop.org/0953-8984/1/3/012>)

View [the table of contents for this issue](#), or go to the [journal homepage](#) for more

Download details:

IP Address: 171.66.16.90

The article was downloaded on 10/05/2010 at 17:00

Please note that [terms and conditions apply](#).

## Phase relations and physical properties of $\text{Li}_2\text{Mg}_{1-r}\text{Cu}_{2-r}\text{O}_{3-r+x}$

J Hauck†, K Bickmann†, B Bischof†, C Freiburg‡, D Henkel†,  
U Köbler†, K Mika†, W Reichert‡, E M Würtz†, S Ipta§ and  
H Altenburg§

† Institut für Festkörperforschung, Kernforschungsanlage, D-5170 Jülich, Federal  
Republic of Germany

‡ ZCH, Kernforschungsanlage, D-5170 Jülich, Federal Republic of Germany

§ FH Münster, Chemieingenieurwesen, D-4430 Steinfurt, Federal Republic of Germany

Received 10 May 1988

**Abstract.**  $\text{Li}_2\text{CuO}_2$  and  $\text{MgCu}_2\text{O}_3$ , isomorphous to superconducting  $\text{TiO}$ , form solid solutions  $\text{Li}_2\text{Mg}_{1-r}\text{Cu}_{2-r}\text{O}_{3-r+x}$  with orthorhombic symmetry at  $0 \leq r \leq 0.25$  and  $0.90 \leq r \leq 1$  and three tetragonal phases  $\alpha$ ,  $\beta$  and  $\gamma$  at  $r = 0.5$  with phase transitions at about 400 and about 800 °C. The O and the Li–Mg sublattices disorder at the  $\alpha$ -to- $\beta$ - and the  $\beta$ -to- $\gamma$ -phase transitions, respectively, in tetragonal phases with lattice constants  $a = 399.3$  pm,  $c = 883.1$  pm ( $\gamma$ ) and  $a = 572.1$  pm,  $c = 1239.5$  pm ( $\alpha$ ). The resistivity of samples is decreased at various  $r$ -values with semiconducting behaviour. The magnetic moment at Cu atoms is  $1.3\mu_B$ – $1.5\mu_B$  per Cu atom.

### 1. Introduction

The superconducting copper oxides  $\text{La}_{2-r}\text{Sr}_r\text{CuO}_{4-x}$ ,  $\text{Ba}_2\text{YCu}_3\text{O}_{6.5+x}$  and also the new  $(\text{Ca}, \text{Sr})_3\text{Bi}_2\text{Cu}_2\text{O}_{8+x}$  can be considered as interstitial alloys  $\text{MZ}_y$  of  $\text{Z} \equiv \text{O}$  atoms at octahedral sites of a BCC derivative M lattice, where  $\text{M} \equiv \text{La}_{2-r}\text{Sr}_r\text{Cu}$ ,  $(\text{MoSi}_2$  alloy structure),  $\text{Ba}_2\text{YCu}_3$  or  $(\text{Ca}, \text{Sr})_3\text{Bi}_2\text{Cu}_2$  [1]. The O coordination of Cu atoms varies from octahedral to fivefold, fourfold or twofold. The present Cu oxides  $\text{Li}_2\text{CuO}_2$  [2] and  $\text{MgCu}_2\text{O}_3$  [3] can also be considered as  $\text{MZ}_y$  interstitial alloys, Z at octahedral sites but with a FCC  $\text{M} \equiv \text{Li}_2\text{Cu}$  or  $\text{MgCu}_2$  lattice with  $\text{MoPt}_2$  alloy structure [1]. Both oxides are isomorphous to  $\text{TiO} \equiv \text{Ti}_2\text{O}_2$  with vacancies  $\square$  in the M and Z sublattices. The Cu atoms of  $\text{MgCu}_2\text{O}_3$  and Li atoms of  $\text{Li}_2\text{CuO}_2$  are on Ti positions of the  $\text{Ti}_2\text{O}_2$  structure [1].  $\text{TiO}$  is superconducting below  $T_c = 2.3$  K [4], while brown-red  $\text{Li}_2\text{CuO}_2$  and grey  $\text{MgCu}_2\text{O}_3$  are non-metallic. The solid solution,  $\text{Li}_2\text{Mg}_{1-r}\text{Cu}_{2-r}\text{O}_{3-r+x}$  ( $0 \leq r \leq 1$ ) of  $\text{Li}_2\text{CuO}_2$  and  $\text{MgCu}_2\text{O}_3$  is similar for example to the  $\text{La}_{2-r}\text{Sr}_r\text{CuO}_{4-r/2+x}$  solid solution [5], where conductivity can be increased by substitution with low-valent M atoms, divalent Sr for trivalent La or monovalent Li for divalent Mg. The  $x = 0$  reference O content  $3 - r$  and  $4 - r/2$  is defined for formally divalent Cu. The  $\text{Ba}_2\text{YCu}_3\text{O}_{6.5+x}$  system had shown that  $x$  can be positive and negative for formally trivalent and monovalent Cu, respectively [6].

## 2. Experimental details

$\text{Li}_2\text{O}$  (obtained from  $\text{LiOH}$  at  $700^\circ\text{C}$  and  $10^{-3}$  bar),  $\text{CuO}$  and  $\text{MgO}$  were mixed in different ratios, sintered at  $700\text{--}1100^\circ\text{C}$  in corundum or  $\text{MgO}$  crucibles. The oxygen partial pressure  $p_{\text{O}_2}$  could be varied from 0.01 to 1 bar by mixing  $\text{O}_2$  and Ar with a gas-mixing pump at a constant flow rate.

The phases of  $\text{Li}_2\text{CuO}_2\text{--MgCu}_2\text{O}_3$  solid solution were characterised by x-ray diffraction (the Bragg–Brentano or Guinier method), differential thermal analysis (DTA), thermogravimetric analysis (TGA), optical microscopy and scanning electron microscopy, resistivity (qualitatively with an ohmmeter and quantitatively with the four-point method at  $10\text{--}300$  K) and susceptibility measurements (with a Faraday balance at  $4\text{--}300$  K). The absolute O content was determined by the difference in weight after  $\text{H}_2$  reduction for 10 h at  $600^\circ\text{C}$  to a  $\text{Li}_2\text{O--MgO--Cu}$  mixture.  $\text{Li}_2\text{CuO}_2$  impurities can be dissolved in aqueous ammonia to give a blue colour while the other phases, except  $\text{Li}_2\text{O}$ , dissolve only in acids.

## 3. Results

$\text{Li}_2\text{CuO}_2\text{--MgCu}_2\text{O}_3$  or  $\text{Li}_2\text{O--MgO--CuO}$  mixtures could be equilibrated to  $\text{MgCu}_2\text{O}_3\text{--Li}_2\text{CuO}_2$  solid solutions after reaction for  $10\text{--}20$  h at about  $1000^\circ\text{C}$ . The reaction of  $\text{MgO}$  and  $\text{CuO}$  is still very sluggish at these temperatures, although some of the  $\text{Li}_2\text{O}$  is volatile and samples with a high  $\text{Li}_2\text{CuO}_2$  content are molten. The reaction of  $\text{Li}_2\text{O--MgO--CuO}$  mixtures at decreased temperatures or shorter annealing times yielded  $\text{Li}_2\text{CuO}_2\text{--CuO--MgO}$  reaction products because of favourable kinetics for  $\text{Li}_2\text{CuO}_2$  formation. At  $1000^\circ\text{C}$ ,  $\text{MgCu}_2\text{O}_3\text{--Li}_2\text{CuO}_2$  forms a solid solution  $\text{Li}_2\text{Mg}_{1-r}\text{Cu}_{2-r}\text{O}_{3-r+x}$  at  $0 \leq r \leq 0.25$  (samples A),  $0.90 \leq r \leq 1$  (samples B) and three modifications  $\alpha$ ,  $\beta$  and at  $0.5 \leq r \leq 0.56$  (samples C).

The solid solution samples A at  $0 \leq r \leq 0.25$  with a  $\text{MgCu}_2\text{O}_3$  structure have a maximum extension at about  $1000^\circ\text{C}$ . At this temperature the  $r = 0.25$  phase forms a eutectic melt with the  $r = 0.5$  phase. The melting point increases to about  $1120^\circ\text{C}$  for samples with low  $r$ . The  $a$  and  $b$  lattice constants of  $\text{MgCu}_2\text{O}_3$  [3]— $a = 400$  pm,  $b = 319$  pm and  $c = 935$  pm—decrease by about 2% at increased  $r = 0.25$  ( $b$  and  $c$  are chosen to be as in the  $\text{Li}_2\text{CuO}_2$  structure [2]).

Samples with  $r > 0.56$  are molten at  $1000^\circ\text{C}$ . Black samples (B) of  $\text{Li}_2\text{CuO}_2$  solid solutions are obtained by cooling the melt after annealing for about 15 h at  $1000^\circ\text{C}$ , whereas mixtures of  $\text{Li}_2\text{CuO}_2$  with unreacted  $\text{MgO--CuO}$  are formed at short annealing times or decreased temperatures. The  $a$  and  $b$  lattice constants of  $\text{Li}_2\text{CuO}_2$  [2]— $a = 366.2$  pm,  $b = 286.3$  pm and  $c = 939.6$  pm—increase by about 1% for the maximum solution of  $\text{MgCu}_2\text{O}_3$ .

Samples C are three tetragonal modifications  $\alpha$ ,  $\beta$  and  $\gamma$  obtained at  $0.5 \leq r \leq 0.56$  with phase transformations at about  $400^\circ\text{C}$  and about  $800^\circ\text{C}$ , depending on the oxygen partial pressure (figure 1). The  $\gamma$ -modification melts congruently at  $1064^\circ\text{C}$ . It can be investigated at room temperature after quenching in liquid nitrogen. The phase transition to  $\beta$ -phase with an enthalpy  $\Delta H_{\beta\gamma}$  of transformation of  $253 \pm 10$  J  $\text{g}^{-1}$  on heating is reversible, e.g. at a decrease of  $50\text{--}100^\circ\text{C}$  in the transition temperatures for a  $5^\circ\text{C min}^{-1}$  cooling process. This phase transition is associated with the ordering of Li and Mg atoms as will be shown from an analysis of different x-ray patterns.

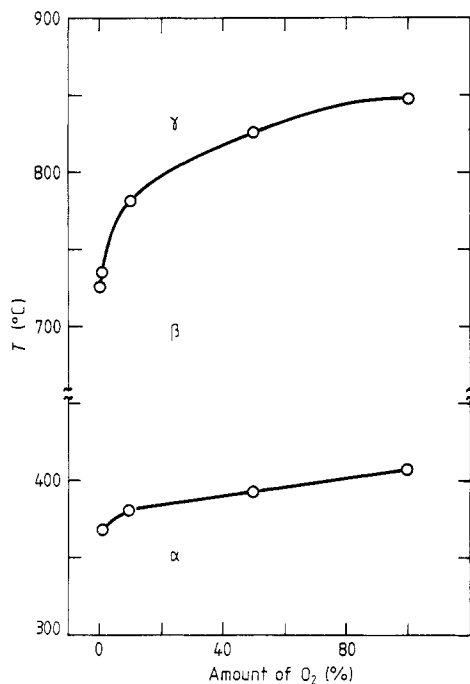


**Figure 1.**  $\alpha$ -to- $\beta$ -to- $\gamma$ -phase transitions of  $\text{Li}_8\text{Mg}_4\text{Cu}_{12}\text{O}_{20+x}$  for different percentages of  $\text{O}_2$  in  $\text{O}_2$ -Ar gas mixtures at 1 bar.

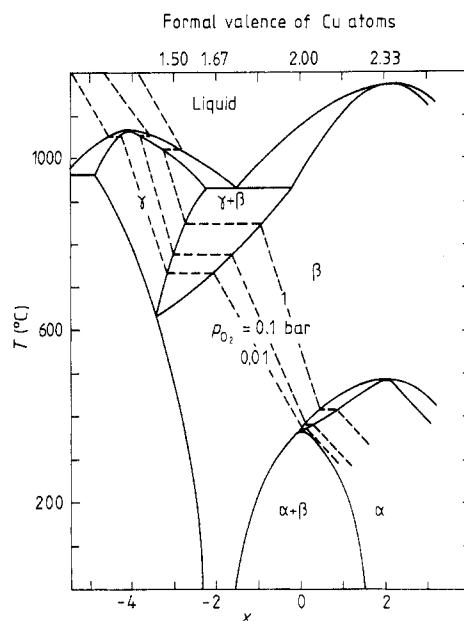
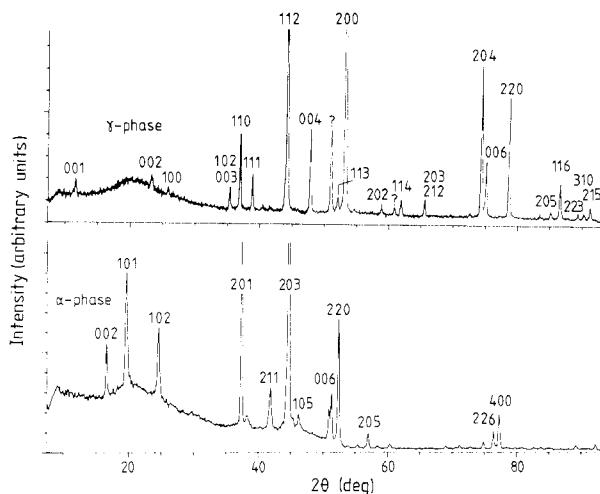


**Figure 2.** Schematic phase diagram of temperature against O content  $x$  of pseudo-binary oxide  $\text{MO}_x$  ( $M \equiv \text{Li}_8\text{Mg}_4\text{Cu}_{12}\text{O}_{20}$ ) at different oxygen partial pressures (---).

The  $\alpha$ -to- $\beta$ -phase transition at about 400 °C seems to be related to the ordering of O atoms. The DTA experiments with varied oxygen partial pressure  $p_{\text{O}_2}$  on consecutive heating and cooling cycles show peaks only on heating with a change  $\Delta H_{\alpha\beta}$  in enthalpy of 4–48 J g<sup>-1</sup>, increasing at increased  $p_{\text{O}_2}$ . No peak was observed while heating in pure Ar. The peak, however, recovered at the appropriate temperature (figure 1) and increased to the usual magnitude after several cycles at increased  $p_{\text{O}_2}$ . This suggests the absence of the phase transition for low O content, as outlined in figure 2. The phase relations for low O contents are similar to those for tetragonal  $\text{Ba}_2\text{GdCu}_3\text{O}_6$ , which does not transform to the orthorhombic phase [6].

The phase transitions of the present system are first order and can be studied by DTA and TGA experiments. The free enthalpy of the ordering process for the  $\alpha$ -to- $\beta$ -phase transitions increases with increasing O content. The TGA shows a step-like decrease in O content in the two-phase regions, which can be explained by phase relations outlined in figure 2. The O content decreases at both phase transitions on heating. The  $\beta$ -to- $\gamma$ -phase transition temperature increases even more markedly with increasing  $p_{\text{O}_2}$  (figure 1) and increasing O content (figure 2) than the  $\alpha$ -to- $\beta$ -phase transition temperature does. The ordering of the Li-Mg sublattice at the  $\beta$ -to- $\gamma$ -phase transition seems to be important for occupation of O vacancies. The TGA experiments at  $p_{\text{O}_2} = 1$  bar show a slightly increased O content in the melt, which can be explained by the phase relations in figure 2. The  $\gamma$ -phase of composition  $\text{Li}_8\text{Mg}_4\text{Cu}_{12}\text{O}_{16}$  with  $x = -4$  decomposes to  $4\text{Li}_2\text{CuO}_2 + 4\text{Cu}_2\text{O} + 4\text{MgO}$  on inappropriate cooling, where kinetics are too slow to

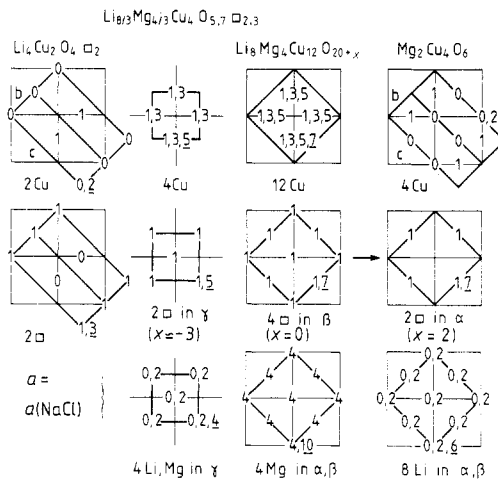
increase the O content. Fast quenching in liquid nitrogen yields the  $\gamma$ -phase powder pattern, very slow cooling ( $3\text{ }^\circ\text{C min}^{-1}$ ) yields the  $\alpha$ -phase, while cooling in air (after removing the quartz tube from the furnace) produces a mixture of  $\alpha$ - and  $\gamma$ -phases and decomposition products. These experiments show that the lower limit of single-phase  $\gamma$  and  $\beta$  should be shifted to increased  $x$  at decreased temperatures (figure 2).



**Figure 3.** X-ray powder pattern (Co  $K\alpha_1$  radiation) for new tetragonal  $\alpha$ - and  $\gamma$ -phases of  $\text{Li}_8\text{Mg}_4\text{Cu}_{12}\text{O}_{20-x}$ .

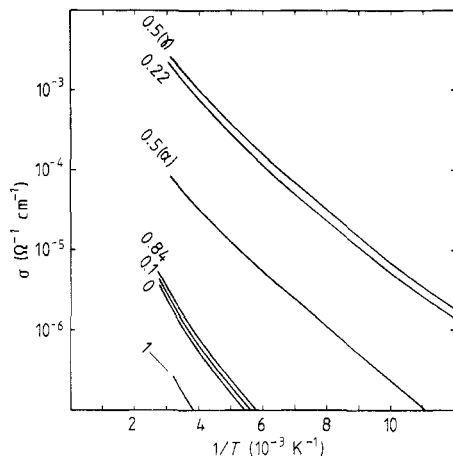
The x-ray powder patterns of  $\alpha$ - and  $\beta$ -phases are very similar because of the weak scattering of O atoms. The pattern of the  $\gamma$ -phase is different (figure 3). The strong 111, 200 and 220 ‘NaCl reflections’ of pseudo-cubic  $\text{MZ}_y$  lattice are split differently for  $\alpha$ - $\beta$ - and  $\gamma$ -phase samples. Tetragonal unit cells were obtained for both patterns:  $a = 399.3\text{ pm}$  and  $c = 883.1\text{ pm}$  for the  $\gamma$ -phase;  $a = 572.1\text{ pm}$  and  $c = 1239.5\text{ pm}$  for the  $\alpha$ -phase (after repeated annealing at  $p_{\text{O}_2} = 1\text{ bar}$ ). The lattice parameters of the  $\alpha$ -phase are slightly increased to  $a = 572.8\text{ pm}$  and  $c = 1239.8\text{ pm}$  on increased cooling rate and therefore decreased O content. The unit cell of the  $\gamma$ -phase is about twice the  $\text{MZ}_y$  NaCl unit cell with eight M- and eight Z-atom positions, while the unit cell of the  $\alpha$ -phase with  $a \approx \sqrt{2}a(\text{NaCl})$  and  $c \approx 3a(\text{NaCl})$  contains 24 M- and 24 Z-atom positions. The composition of M and Z can be obtained from the  $r$ -values of single-phase  $\text{Li}_{2r}\text{Mg}_{1-r}\text{Cu}_{2-r}\text{O}_{3-r+x}$ :  $\text{Li}_{2.67}\text{Mg}_{1.33}\text{Cu}_4\text{O}_{6.67+x}$  at  $r = 0.5$  and  $\text{Li}_3\text{Mg}_{1.17}\text{Cu}_{3.83}\text{O}_{6.5+x}$  at  $r = 0.56$  for the  $\gamma$ -phase;  $\text{Li}_8\text{Mg}_4\text{Cu}_{12}\text{O}_{20+x}$  ( $r = 0.5$ ) and  $\text{Li}_9\text{Mg}_{3.5}\text{Cu}_{11.5}\text{O}_{19.5+x}$  ( $r = 0.56$ ) for the  $\alpha$ -phase. The  $r = 0.5$  composition agrees with onefold, twofold, fourfold, eightfold and 16-fold positions at tetragonal symmetry. At  $r = 0.56$  about 4% of the Cu atoms should be substituted by Mg atoms. However, the observation of identical phase transition temperatures (figure 1) for samples with nominally different  $r$ -values suggests negligible Mg substitution and therefore a constant  $r = 0.5$  composition of the  $\alpha$ -,  $\beta$ - and  $\gamma$ -phases. The increased Li content at  $r = 0.5$ – $0.56$  is probably volatile during the annealing process. The oxygen content  $x = -3$  ( $\gamma$ -phase) and  $x = 2$  ( $\alpha$ -phase) correspond to two monovalent and two divalent Cu atoms in  $\gamma$ - $\text{Li}_{2.67}\text{Mg}_{1.33}\text{Cu}_4^{\frac{1}{2}}\text{Cu}_2^{\frac{2}{2}}\text{O}_{5.7}$ , and four trivalent and eight divalent Cu atoms in  $\alpha$ - $\text{Li}_8\text{Mg}_4\text{Cu}_8^{\frac{2}{3}}\text{Cu}_4^{\frac{2}{2}}\text{O}_{22}$ . All Cu atoms are divalent at  $x = 0$  (figure 2).

Figure 4 shows the ordering of Li, Mg, Cu and O atoms in agreement with the observed tetragonal symmetry. Other configurations are possible—in particular for Li and O atoms in the  $\alpha$ - and  $\beta$ -phase, which is difficult to determine by x-ray diffraction. The suggested ordering of Li atoms and O vacancies  $\square$  is similar to that in  $\text{Li}_2\text{CuO}_2\square$  [2]. The O vacancies  $\square$  in  $\text{Li}_2\text{CuO}_2\square$  are in the sequence  $\square\text{-Cu}\text{-}\square\text{-Cu}$  in the  $a$  axis direction (figure 4), so that all Cu atoms have planar fourfold O coordination. In  $\alpha\text{-Li}_8\text{Mg}_4\text{Cu}_{12}\text{O}_{22}\square_2$  with a sequence  $\text{O}\text{-Cu}\text{-O}\text{-Cu}$  in the  $c$  axis direction, eight  $\text{Cu}^{2+}$  atoms have octahedral and four  $\text{Cu}^{3+}$  atoms have fourfold planar O coordination. The  $\text{Cu}^+$  atoms in the  $\gamma$ -phase and  $\beta$ -phase at low  $x$  have twofold coordinations in the suggested structure (figure 4). The relative distance between Cu atoms decreases from  $c/2a = 1.11$  in the  $\gamma$ -phase to  $c\sqrt{2}/3a = 1.02$  in the  $\alpha$ -phase—about 0.90 in  $\text{MgCu}_2\text{O}_3$  and about 0.87 in  $\text{Li}_2\text{CuO}_2$ . In  $\alpha$ -,  $\beta$ - and  $\gamma$ -phases and  $\text{Li}_2\text{CuO}_2$  the Li atoms, which are close to the O vacancy positions, have smaller coordination numbers. The fourfold coordination in  $\text{Li}_2\text{CuO}_2$  is tetrahedral [2]. The unit-cell content of the  $\gamma$ -phase ( $\text{Li}_{2.67}\text{Mg}_{1.33}\text{Cu}_4\text{O}_{6.67+x/3}$  with  $x \approx -3$ ) suggests a disorder of Li–Mg and part of the O sublattice. 71% of the total O positions are occupied in the  $\gamma$ -phase, 83% in the  $\alpha$ - and  $\beta$ -phases at  $x = 0$ , and 92% in the  $\alpha$ -phase at  $x = 2$ . The  $x = 0$  composition is similar to that for 83% occupation of the  $Z \equiv C$  positions in ordered or disordered  $\text{V}_6\text{C}_5\square$  or  $\text{Nb}_6\text{C}_5\square$  [1]. The C atoms of the disordered phase have short-range order, whereas the ordered phases have some disorder. This might be similar in the present system.



**Figure 4.** Projection of Cu, Mg, Li atoms and O vacancy  $\square$  positions in  $\text{Li}_2\text{Cu}_2\text{O}_4\square_2\text{-Mg}_2\text{Cu}_4\text{O}_6$  neglecting distortions [2, 3] and  $\alpha$ -,  $\beta$ - and  $\gamma$ - $\text{Li}_8\text{Mg}_4\text{Cu}_{12}\text{O}_{20+x}$  unit cells on an NaCl lattice grid with  $a(\text{NaCl}) = 2$ . The underlined numbers show the periodicity in height.

Grey  $\text{MgCu}_2\text{O}_3$  and reddish brown  $\text{Li}_2\text{CuO}_2$  are insulating. The electrical resistivity decreases in the black samples of solid solutions A, B and C. All samples investigated so far show increased conductivity but are still semiconducting (figure 5). Magnetic measurements of the susceptibility were performed at 4–300 K for the  $\alpha$ -phase. The data can be fitted to Curie–Weiss laws with  $\mu_{\text{eff}} = 1.3\mu_{\text{B}}\text{-}1.5\mu_{\text{B}}$  per Cu atom and  $\theta$  in the range from  $-31$  to  $-40$  K. A very small contribution from Pauli paramagnetism and the observed magnetic moment indicate localisation of the electrons in the  $d^9$  configuration



**Figure 5.** Conductivity of  $\text{Li}_2\text{Mg}_{1-r}\text{Cu}_{2-r}\text{O}_{3-r+x}$  samples with different  $r$ -values (shown as curve labels).

of divalent Cu. The magnetic moments do not order above 4 K.  $\text{Li}_2\text{CuO}_2$  and  $\text{MgCu}_2\text{O}_3$  have  $\mu_{\text{eff}} = 1.9$  and  $>0.8 \mu_{\text{B}}$  per Cu atom and order at the Néel temperatures  $10$  and  $70 \pm 0.5$  K, respectively.

#### 4. Conclusion

$\text{Li}_2\text{CuO}_2\Box$  and  $\text{MgCu}_2\text{O}_3$  form solid solutions with the formula  $\text{Li}_2\text{Mg}_{1-r}\text{Cu}_{2-r}\text{O}_{3-r+x}$  at  $0 \leq r \leq 0.25$  (samples A),  $0.90 \leq r \leq 1$  (samples B) and three modifications  $\alpha$ ,  $\beta$  and  $\gamma$  at  $r = 0.5$  (samples C). There are miscibility gaps at  $0.25 \leq r \leq 0.50$  and  $0.50 \leq r \leq 0.90$ . The metal sublattice can be considered to be FCC derivative structures:  $\text{M} \equiv \text{MgCu}_2$  for  $\text{MgCu}_2\text{O}_3$  solid solution (samples A) and  $\text{M} \equiv \text{Li}_2\text{Cu}$  for  $\text{Li}_2\text{CuO}_2$  solid solution (samples B) have an orthorhombic  $\text{MoPt}_2$  alloy structure, and  $\text{M} \equiv (\text{Li}_2\text{Mg})\text{Cu}_3$  for  $\alpha$ -,  $\beta$ - and  $\gamma$ -phases (samples C) have a  $\text{CuAu}$  alloy structure (figure 4). The  $\text{Li}_2\text{Mg}$  sublattice is disordered in the  $\gamma$ -phase with tetragonal unit-cell lattice constants  $a = 399.3$  pm and  $c = 883.1$  pm and ordered in the tetragonal  $\beta$ -phase with  $a = 572.1$  pm ( $\approx \sqrt{2}a(\text{NaCl})$ ) and  $c = 1239.5$  pm. The O sublattice orders below about  $400^\circ\text{C}$  in the  $\alpha$ -phase.

$\text{Li}_2\text{Mg}_{1-r}\text{Cu}_{2-r}\text{O}_{3-r+x}$  samples A and B can be compared with the solid solution  $\text{La}_{2-r}\text{Sr}_r\text{CuO}_{4-r/2+x}$ , where the symmetry of the phases is maintained in certain ranges, e.g. the orthorhombic phase for  $0 \leq r \leq 0.16$  and the tetragonal phase for  $0.16 \leq r \leq 0.5$  [5]. Samples A and B in the present system have different O contents.  $\text{MgCu}_2\text{O}_3$  solid solution samples consist of  $\text{CuO}_6$  octahedra, which are linked by apices and edges, whereas Cu atoms of  $\text{Li}_2\text{CuO}_2\Box$  have a planar coordination of four O neighbours forming  $\text{CuO}_2$  chains in the  $b$  axis direction (figure 4). The chains are linked by edges, whereas  $\text{CuO}_4$  groups of Cu(1) atoms in  $\text{Ba}_2\text{YCu}_3\text{O}_7$  are linked at apices.

The  $\alpha$ -,  $\beta$ - and  $\gamma$ -phases with  $r = 0.5$  (samples C) can be compared with the  $\text{Ba}_2\text{YCu}_3\text{O}_{6.5+x}$  system. The ratio of  $\text{Li} : \text{Mg} : \text{Cu} = 2 : 1 : 3$  is constant, while the O content  $x$  in  $\text{Li}_8\text{Mg}_4\text{Cu}_{12}\text{O}_{20+x}$  can vary between  $-4$  and  $2$  as outlined in figure 2. The  $\alpha$ -to- $\beta$ -phase transition at about  $400^\circ\text{C}$  is probably absent at low O contents, as in tetragonal  $\text{Ba}_2\text{GdCu}_3\text{O}_6$  which does not transform to the orthorhombic phase [6]. The Li-Mg sublattice becomes disordered at the  $\beta$ -to- $\gamma$ -phase transition at about  $800^\circ\text{C}$ ; this might

be due to the small size and high mobility of Li atoms. The lattice constants  $c = 2a(\text{NaCl})$  ( $\gamma$ -phase) and  $c = 3a(\text{NaCl})$  ( $\alpha$ -phase) are related to alternating  $\text{Cu}^+-\text{Cu}^{2+}$  layers ( $\gamma$ -phase with  $x = -3$ ) and  $\text{Cu}^{3+}-\text{Cu}^{2+}-\text{Cu}^{2+}$  layers ( $\alpha$ -phase with  $x = 2$ ).

Despite the large variety of phases in the  $\text{Li}_2\text{Mg}_{1-r}\text{Cu}_{2-r}\text{O}_{3-r+x}$  system and some analogies to superconducting  $\text{Ba}_2\text{YCu}_3\text{O}_{6.5+x}$  or  $\text{La}_{2-r}\text{Sr}_r\text{CuO}_{4-r/2+x}$ , the physics of the present system seem to be quite simple. All samples investigated so far are semiconducting. Measurements of magnetic properties show that the d electrons of divalent Cu atoms are localised in  $d^9$  configuration without magnetic ordering above 4 K.

A physical property concerning the mechanical strength, namely the deterioration of bulk material after repeated loading and unloading with O seems to be new in oxide systems but is well known for interstitial alloys, e.g.  $\text{FeTiH}_x$  [7]. The variation in volume of about 3.7% at the  $\beta$ -to- $\gamma$ -phase transition (figures 1 and 2) causes internal strain. Large grains of the starting material for DTA and TGA runs at different  $p_{\text{O}_2}$ -values (figures 1 and 2) deteriorated to a fine powder after several cycles of O loading and unloading.

## References

- [1] Hauck J, Henkel D and Mika K 1988 *J. Magn. Magn. Mater.* **76 + 77** at press
- [2] Hoppe R and Riek H 1970 *Z. Anorg. Allg. Chem.* **379** 157
- [3] Drenkhahn H and Müller-Buschbaum H 1975 *Z. Anorg. Allg. Chem.* **418** 116
- [4] Doyle N J, Hulm J K, Jones C K, Miller R C and Taylor A 1968 *Phys. Lett.* **26A** 604
- [5] Nguyen N, Studer F and Raveau B 1983 *J. Phys. Chem. Solids* **44** 389
- [6] Hauck J, Bickmann K and Zucht F 1987 *Z. Phys.* **B 67** 299
- [7] Wenzl H 1982 *Int. Metall. Rev.* **27** 140